

Mechanical Properties and the Microstructure of $\text{Al}_2\text{O}_3/\text{Al}/\text{Al}_2\text{O}_3$ Joints with the Surface Modification of Alumina by a Thin Layer of Ti + Nb

Marzanna Ksiazek, Adam Tchorz, and Lukasz Boron

(Submitted November 19, 2013; in revised form March 18, 2014; published online April 18, 2014)

$\text{Al}_2\text{O}_3/\text{Al}/\text{Al}_2\text{O}_3$ joints were formed by liquid-state bonding of alumina substrates covered with a thin Ti + Nb coating of 900 nm thickness with the use of an Al interlayer of 30 μm at 973 K under a vacuum of 0.2 mPa for 5 min. The bond strength of the joints was examined by a four-point bending test at 295, 373, and 473 K. Optical, scanning, and transmission electron microscopies were applied for detailed characterization of the interface structure and failure characteristics of fractured joint surfaces. The analysis of the results has shown that (i) bonding occurred due to the formation of a reactive interface on the metal side of the joint in the presence of $\text{Al}_3\text{Nb}(\text{Ti})$ precipitates and (ii) modification of Al_2O_3 by a thin layer of Ti + Nb increases the hardness at the interface and makes it possible to achieve reliable joints working at elevated temperatures.

Keywords coatings, joining, surface engineering

1. Introduction

The metal/ceramic joint showed a series of unique properties that do not occur in any other material in such a combination. The applicability and occupied time of the final metal/ceramic joints depend on the dissipation of the stress concentration, which increases the ceramic's cracking strength in the formation of such interatomic bonds that will ensure obtaining a durable and reliable joint. The reliability of this joint depends on the interfacial properties between the metal and ceramic, e.g., adhesion properties and thermal stability. However, the differences in physical and chemical characteristics between the metal and ceramics cause severe changes in the region of the interface (a discontinuous change in the elastic, plastic, and thermal characteristics at the interface), and the difference between the values of linear coefficients of the thermal expansion of the metal and ceramic leads to the formation of residual stress at the interface. That is why in order to identify the optimum mechanical integrity of the metal/ceramic joint, one shall consider a number of factors: the process of the bond formation, chemical composition, morphology and the structure of the metal/ceramic joint, thermal area and plastic

incompatibility, the limit value of the metal strength and its thickness (it determines the distribution of residual stress and the stress occurring currently at the joint load), the number of defects in a ceramic material and at the interface, and also the resistance of the interfacial region to cracking (it determines the course of the cracking path) (Ref 1-4).

The phenomena occurring at the contact of liquid and solid phase have a decisive influence on the process of joining these materials. The most important ones include wetting of the ceramic material surface by liquid metal and mutual chemical interaction between the liquid metal and ceramic, related with diffusion processes. The reactivity and wetting behavior in a metal/ceramic system can in turn be improved, e.g., by applying thin metallic layers to the ceramic material surface (Ref 5, 6). Such layers can be reactive against the bonded materials so that a fixed bond on the phase boundaries is formed, creating diffusion, reactive intermediate microlayers in the most favorable case; the layers have a physical and chemical compatibility (thermodynamic and kinetic), which guarantees good mechanical characteristics of the joint. A number of studies focus on research of the influence between pure titanium and Al_2O_3 together with the definition of the morphology of the reaction area which is created at the interface of $\text{Ti}/\text{Al}_2\text{O}_3$. Kelkar et al. in their study (Ref 7) on the basis of thermodynamic calculations present a concept that the influence between liquid Al and titanium covering Al_2O_3 in a vacuum, even at low partial pressures of oxygen, leads to changes in the chemical composition of the interface at the side of the substrate by forming the following reaction layer: $\text{Al}/\text{Al}_2\text{O}_3/\text{Ti}_x\text{O}_y/\text{Ti}/\text{Ti}_x\text{O}_y/\text{Al}_2\text{O}_3$.

In the previous work (Ref 8), experimental results revealed that the addition of Ti and Nb improves the wetting; titanium influences the contact angle more than niobium (probably because it has a higher chemical affinity to oxygen); and at a thin layer less than 1 μm , the minimal contact angle was reached (40° for titanium and 108° for niobium at 1223 K).

The aim of this work was to study the effect of the Ti + Nb thin film on alumina on the interface structure, bond strength

This article is an invited submission to JMEP selected from presentations at the Symposia “Wetting,” “Interface Design,” and “Joining Technologies” belonging to the Topic “Joining and Interface Design” at the European Congress and Exhibition on Advanced Materials and Processes (EUROMAT 2013), held on September 8-13, 2013, in Sevilla, Spain, and has been expanded from the original presentation.

Marzanna Ksiazek, Adam Tchorz, and Lukasz Boron, Foundry Research Institute, Zakopiańska 73, 30-418 Kraków, Polska. Contact e-mail: marzanna.ksiazek@iod.krakow.pl.

properties at room and elevated temperatures, and the mechanism of destruction of $\text{Al}_2\text{O}_3/\text{Al}/\text{Al}_2\text{O}_3$ joints.

2. Experimental Procedure and Materials

The $\text{Al}_2\text{O}_3/\text{Al}/\text{Al}_2\text{O}_3$ joints were produced by liquid-state bonding of 98% pure polycrystalline Al_2O_3 blocks ($14 \times 14 \times 20$ mm) and 99.99% pure aluminum of 30 μm thick layer.

Foils of the metal (14×14 mm dimensions) were placed between the alumina blocks, and bonding was performed at 973 K with a vacuum of 0.2 mPa for 5 min. The heating and cooling rates used were 30 and 10 min, respectively. The alumina blocks of 3.8 g/cm^3 (almost 0% porosity) were produced by sintering at the temperature of 1923 K for 2 h; powders have the following starting composition: 99.9085% α - Al_2O_3 , 0.009% CaO, 0.053% SiO_2 , 0.0029% MgO, 0.023% Fe_2O_3 , and 0.0036% Na_2O . The polycrystalline alumina contained 2% of $\text{Mg}(\text{SiO}_4)$ and MgAl_2O_4 spinels. The Al foil was mechanically and ultrasonically cleaned in acetone, rinsed in alcohol for 10 min, and then dried with warm air directly before bonding. The Al foils were positioned between two Al_2O_3 blocks, and this assembly was placed in a vacuum chamber under a load applied by placing one of the Al_2O_3 blocks on top of the assembly to maintain structural integrity during bonding.

The surfaces to be joined were lapped flat to a 1- μm finish, ultrasonically cleaned in acetone, and finally a 900-nm-thin Ti + Nb layer was deposited on the surface by physical vapor deposition (PVD). The film was deposited by rf sputtering of a mosaic Ti + Nb target in argon gas atmosphere onto different substrates such as Corning glasses and alumina, depending on the requirements imposed by further applications, i.e., for the determination of the film thickness and composition. The film thickness was measured mechanically by means of a Tally Step profilometer. Research with the use of a scanning electron microscope revealed that the thin layer is smooth and nonporous and that it contains both Ti and Nb. The thin film composition was determined from X-ray diffraction (XRD). The weight ratio $\text{Nb}/(\text{Nb} + \text{Ti})$ was found to be equal to 0.625 (62.5 wt.%).

After bonding, the joints were tested at 295, 373, and 473 K, using the four-point bending test with an inner span of 12.5 and outer span of 25 mm. Specimens of dimensions $3 \times 3 \times 36$ mm^3 for the four-point bend testing were cut from one bonded sample. The specimens were tested using an INSTRON 1115 machine with the automatic recording of the applied load versus the corresponding displacement up to failure under a constant load displacement rate of 1 mm/min. The reported results are averages of between three and five tests that were run for each condition. The impact of temperature was analyzed within the range of 295–473 K on the course of joint's bending characteristics, due to the fact that in practice deformation at a temperature (above 0.25 of melting point) is used to minimize the deformation resistance and increase the plasticity of brittle materials.

The structure was examined on sandwich specimens after joining, using optical microscopy (LM), scanning electron microscopy (SEM), and transmission electron microscopy (TEM). LM/SEM studies were performed on fractured joint specimens, cross sectioned in a plane inclined at about 25° to the joint surface (to enable the enlargement of the joint area available for examinations; it is noted that this technique lowers somewhat the spatial resolution of EDS composition line scans). Moreover, SEM/EDS studies were performed to study failure characteristics of fractured joint surfaces.

The specimens for TEM examination (Model PHILIPS CM20 TWIN operated at 200 KV) were prepared using a method for the preparation of coated material by sandwiching described in detail in (Ref 9) (comprising specimen preparation, bonding together by epoxy glue, mounting, mechanical pre-thinning, and thinning by ion-beam milling until perforation).

3. Results and Discussion

The four-point bending test results of the ceramic-metal-ceramic joints bonded at 973 K are summarized in Fig. 1 for $\text{Al}_2\text{O}_3/\text{Al}/\text{Al}_2\text{O}_3$ and $\text{Al}_2\text{O}_3/\text{Ti} + \text{Nb}/\text{Al}/\text{Ti} + \text{Nb}/\text{Al}_2\text{O}_3$ joints, where the bending strengths are reported at 295, 373, 473 K. Together with the increase of temperature, the force parameters of the bending process decrease and increase the values of bend arrows in the samples, whereas a change in temperature from 295 to 373 and 473 K for sample types $\text{Al}_2\text{O}_3/\text{Al}/\text{Al}_2\text{O}_3$ causes a dramatic change both in stress and in the shape of the bending curve. Maximum bending stress at $T = 473$ K decreases twofold, while $\text{Al}_2\text{O}_3/\text{Ti} + \text{Nb}/\text{Al}/\text{Ti} + \text{Nb}/\text{Al}_2\text{O}_3$ joints in the tested temperature range maintain the same character of the bending curve, which in turn proves the same character of the deformation mechanism at the room temperature and elevated temperature. Specimens of types $\text{Al}_2\text{O}_3/\text{Al}/\text{Al}_2\text{O}_3$ and $\text{Al}_2\text{O}_3/\text{Ti} + \text{Nb}/\text{Al}/\text{Ti} + \text{Nb}/\text{Al}_2\text{O}_3$ at 295 K displayed an average breaking stress with a standard deviation of about 10 MPa, while specimens of the same type at 373 and 473 K had a standard deviation of about 15 MPa. At 295 K, the standard deviation was smaller, and its value increased together with the increase of temperature during the examination. The increase of the standard deviation may indicate a more complex character of damaging the sample, which by nature influences more extended distribution of strength tests. It has been shown that the bending strengths of metal-ceramic joints with Ti + Nb coating have been improved compared to those joints without coatings at elevated temperature. Furthermore, it was found that $\text{Al}_2\text{O}_3/\text{Ti} + \text{Nb}/\text{Al}/\text{Ti} + \text{Nb}/\text{Al}_2\text{O}_3$ joints retained its strength to higher temperatures. The bending strength of $\text{Al}_2\text{O}_3/\text{Al}/\text{Al}_2\text{O}_3$ was about 158 ± 15 and 125 ± 15 MPa, while the strength of $\text{Al}_2\text{O}_3/\text{Ti} + \text{Nb}/\text{Al}/\text{Ti} + \text{Nb}/\text{Al}_2\text{O}_3$ was 185 ± 15 and 158 ± 15 MPa at 373 and 473 K, respectively. On the other hand, the bending strength of $\text{Al}_2\text{O}_3/\text{Ti} + \text{Nb}/\text{Al}/\text{Ti} + \text{Nb}/\text{Al}_2\text{O}_3$ joint is much lower than $\text{Al}_2\text{O}_3/\text{Al}/\text{Al}_2\text{O}_3$ joint, wherein the bending curve has better plasticity behavior at 295 K. The prime role of such plasticity is to accommodate the mismatched thermal contractions of the Al_2O_3 and metal.

The significant increase in the bend stress of $\text{Al}_2\text{O}_3/\text{Ti} + \text{Nb}/\text{Al}/\text{Ti} + \text{Nb}/\text{Al}_2\text{O}_3$ joint compared to the values of $\text{Al}_2\text{O}_3/\text{Al}/\text{Al}_2\text{O}_3$ joint at elevated temperatures may be the result of changes in chemistry of the region of interface, which lead to generating a favorable gradient structure type $\text{Al}(\text{Nb},\text{Ti}) + \text{Al}_3(\text{Nb},\text{Ti})/\text{Al}_2\text{O}_3$ and thus lead to increased strength, and in the interaction between interfacial precipitates and dislocations during deformation at the bonding interface which causes the higher yield strength. Such interfacial structure in $\text{Al}_2\text{O}_3/\text{Ti} + \text{Nb}/\text{Al}/\text{Ti} + \text{Nb}/\text{Al}_2\text{O}_3$ joint provides a gradual transition in physical properties and help minimize the effect of local stresses that develop from the mismatch between the coefficient of thermal expansion of Al_2O_3 and the bonding layer of Al (containing Nb and Ti).

The fracture modes of the $\text{Al}_2\text{O}_3/\text{Ti} + \text{Nb}/\text{Al}/\text{Ti} + \text{Nb}/\text{Al}_2\text{O}_3$ joints also differ from that of $\text{Al}_2\text{O}_3/\text{Al}/\text{Al}_2\text{O}_3$. Figure 2 presents

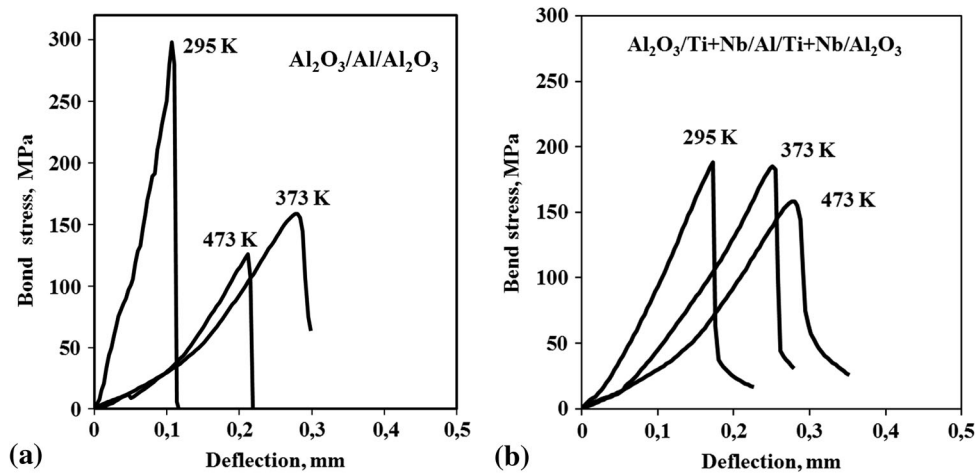


Fig. 1 Bend test curves recorded for (a) $\text{Al}_2\text{O}_3/\text{Al}/\text{Al}_2\text{O}_3$ and (b) $\text{Al}_2\text{O}_3/\text{Ti+Nb}/\text{Al}/\text{Ti+Nb}/\text{Al}_2\text{O}_3$ joints at 295, 373, and 473 K

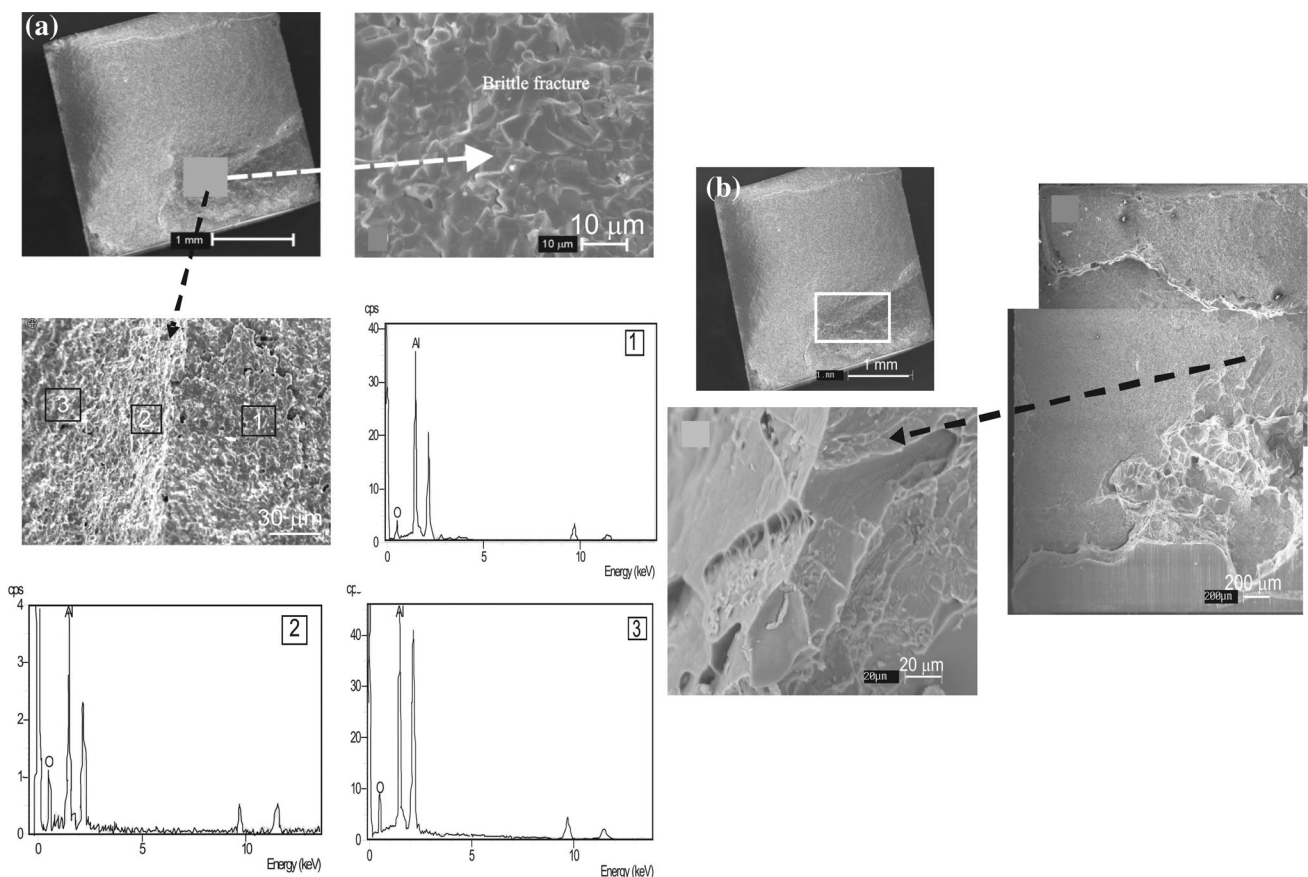


Fig. 2 SEM micrographs of fracture surface after bend test at 295 K (a) of $\text{Al}_2\text{O}_3/\text{Al}/\text{Al}_2\text{O}_3$ joint with corresponding EDS spectrum taken from the marked points 1, 2, and 3, and (b) of $\text{Al}_2\text{O}_3/\text{Ti+Nb}/\text{Al}/\text{Ti+Nb}/\text{Al}_2\text{O}_3$ joint

images of the fracture surfaces resulting from the bending test at 295 K. As illustrated in Fig. 2, two types of fracture modes exist in the ceramic-to-metal joints without and with Ti + Nb coating. In type I, the crack exists in the ceramic during initiating and propagating periods. In joints $\text{Al}_2\text{O}_3/\text{Al}/\text{Al}_2\text{O}_3$, brittle fractures occur along the cleavage planes of the Al_2O_3 phase. This indicates that the bonding strength of $\text{Al}/\text{Al}_2\text{O}_3$ interface is higher than that of the Al_2O_3 . The region of $\text{Al}/\text{Al}_2\text{O}_3$ interface

is "clean" without segregants and reaction products; they tend to be detrimental as it can form brittle compounds. In type II (for the $\text{Al}_2\text{O}_3/\text{Ti+Nb}/\text{Al}/\text{Ti+Nb}/\text{Al}_2\text{O}_3$ joints) cracking occurs both in the metal near the interface and along the interface, which suggests that this region represents the combination of the solid solution and precipitation strengthening (associated with the presence of intermetallics and of Al-rich solid solution, resulting from dissolution of coatings).

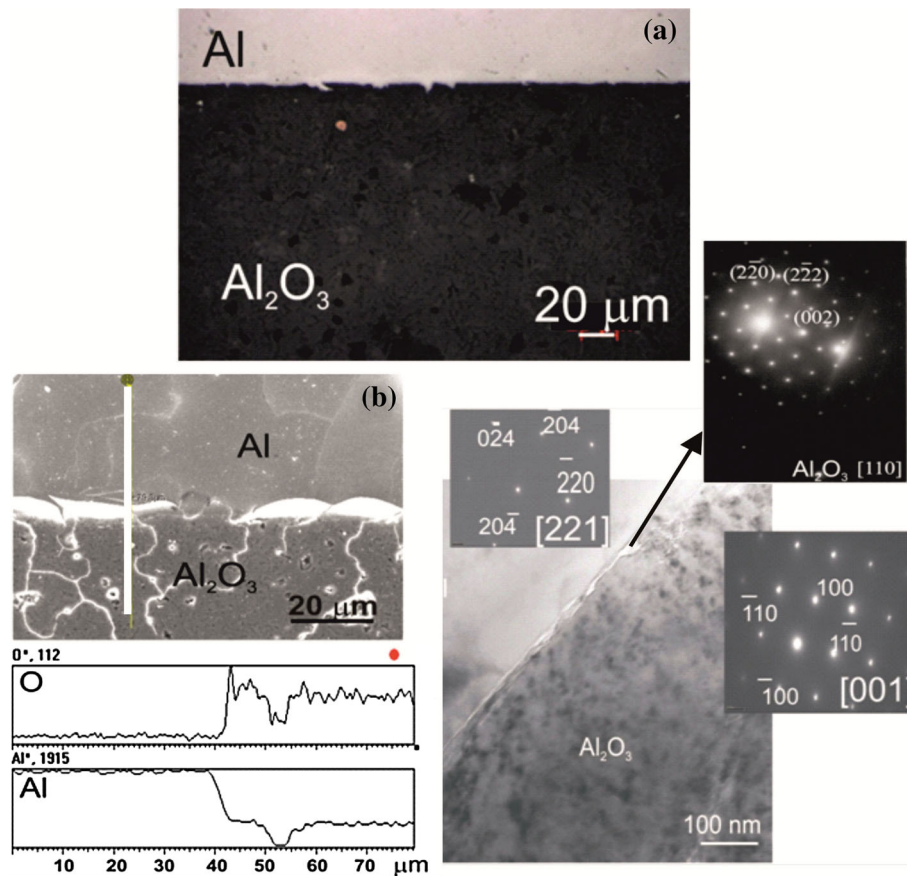


Fig. 3 Structural examination of the $\text{Al}_2\text{O}_3/\text{Al}/\text{Al}_2\text{O}_3$ joint: (a) optical micrograph, (b) SEM analysis of the interface: distribution of O and Al along white line marked in (b), (c) TEM analysis of the interface with representative selected area diffraction patterns indicates the Al and Al_2O_3 phases

For the explanation of the mechanism controlling the bonding process in $\text{Al}_2\text{O}_3/\text{Ti} + \text{Nb}/\text{Al}/\text{Ti} + \text{Nb}/\text{Al}_2\text{O}_3$ joints, the structural examinations were carried out in the region of Al/Ti + Nb/ Al_2O_3 bond by the method of optical microscopy, combined with SEM and TEM, shown in Fig. 3 and 4.

The bonding between Al_2O_3 and Al layer was achieved by growing the Al_2O_3 phase at the interface. The presence of isolated separate particles of Al_2O_3 was confirmed experimentally by SEM/TEM studies in the region of the interface in $\text{Al}_2\text{O}_3/\text{Al}/\text{Al}_2\text{O}_3$ joint (Fig. 3). SEM analysis of the fracture surface of this joint (Fig. 2a) also confirms the presence of Al_2O_3 phases at the interface. It is obvious that oxygen plays an important role in improving the bond strength between Al and Al_2O_3 , probably because of the formation of metal clusters (Ref 10) and chemical interaction between liquid Al and additives in ceramic (Ref 11). At a temperature below 1373 K, through a reduction reaction of silico-aluminate spinels by liquid Al, it is possible to form Al_2O_3 precipitates at the interface, which in turn is conducive to reinforcement of the interface. Therefore, the microstructure of the joint shows a strong bonding at the interfaces. Bend testing at 295 K showed that fractures always occurred within the ceramic material.

Observations of the Al/Ti + Nb/ Al_2O_3 system interface under a magnification of $500\times$ revealed the presence of interfacial precipitates, along the interface (Fig. 4). SEM observations

(Fig. 4b) have proved the formation of new phases, i.e., a phase containing mainly Nb and Ti. The local analysis of the chemical composition of the above-mentioned precipitates has indicated that these are the precipitates of intermetallic phases rich in Nb and Ti (e.g., items 1, 2, and 3 in Fig. 4b, respectively). The chemical composition in the interface region also shows maps of the distribution of the elements like aluminum, titanium, and niobium (Fig. 4b).

Moreover, the last statement was confirmed experimentally by TEM studies of the Al/Ti + Nb/ Al_2O_3 system interface and the presence of particles of $\text{Al}_3\text{Nb}(\text{Ti})$ in the region of interface (Fig. 4c). The structural analysis of the Al/Ti + Nb/ Al_2O_3 bond interfaces produced in the joining process at 973 K indicates that the joining effect has been accompanied by intense chemical interaction between the Ti + Nb film-coated substrate and liquid aluminum. The mechanism of this interaction is probably solution-precipitation based and is related to the dissolution of Ti + Nb coating in liquid aluminum and the formation of a solid solution Al(Nb,Ti) in the contact region during the process of bonding. However, the precipitates of phases rich in Nb and Ti nucleate at the distance of approx. $5\ \mu\text{m}$ from the interface from the supersaturated Al(Nb,Ti) solution, during the cooling of the joint to the ambient temperature (Ref 12).

Figure 5 illustrates the fracture surface of $\text{Al}_2\text{O}_3/\text{Ti} + \text{Nb}/\text{Al}/\text{Ti} + \text{Nb}/\text{Al}_2\text{O}_3$ joints after bending test at elevated

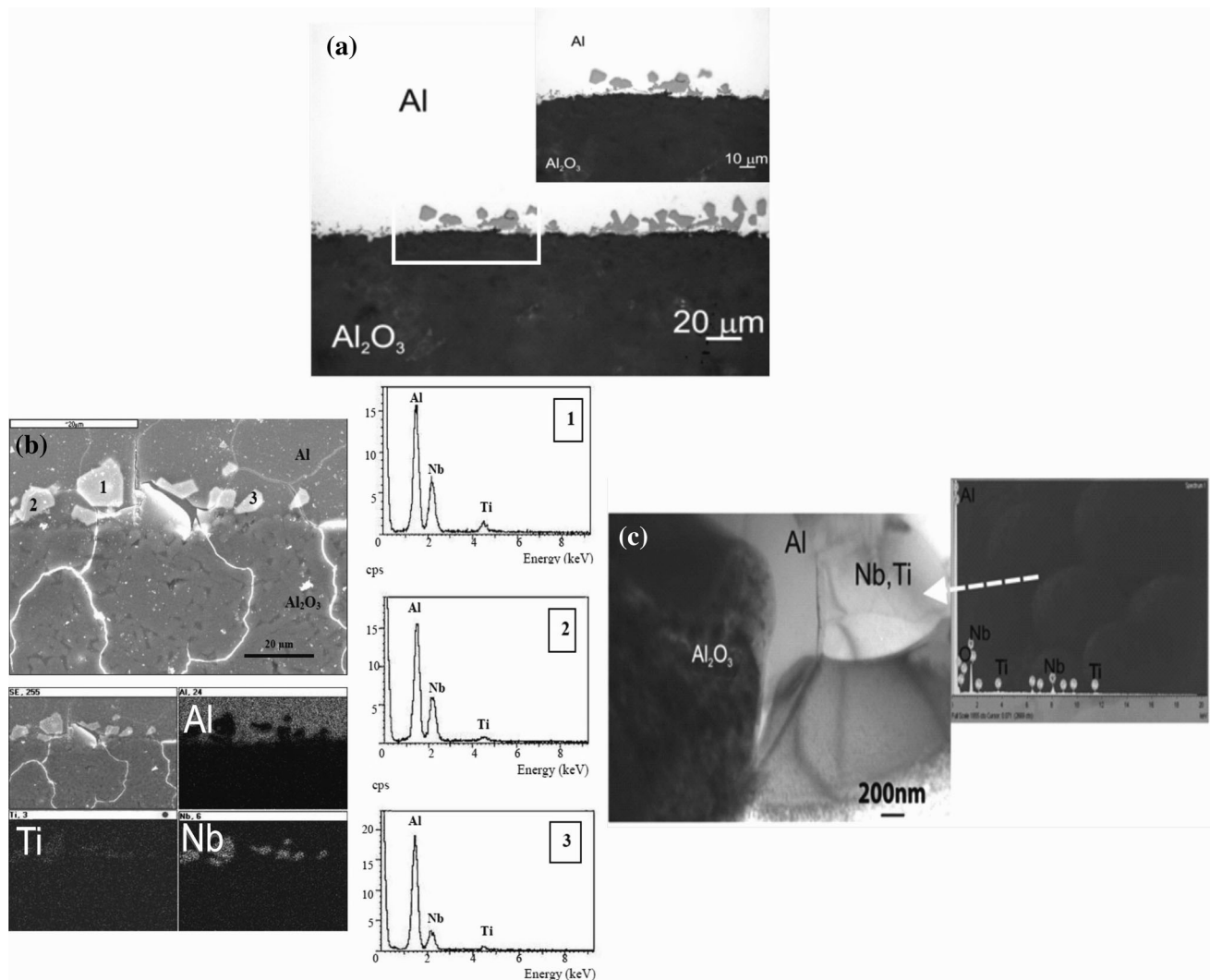


Fig. 4 Structural examination of the $\text{Al}_2\text{O}_3/\text{Ti} + \text{Nb}/\text{Al}/\text{Ti} + \text{Nb}/\text{Al}_2\text{O}_3$ joint: (a) optical micrograph showing the reaction layer in the interfacial region, (b) SEM analysis of the interface with corresponding EDS spectrum taken from the marked points 1, 2, 3, and titanium, aluminum, and niobium X-ray maps and (c) TEM analysis of the interface showing a new phase containing Nb and Ti

temperatures. According to this figure, the fracture preceded in the metal layer near the metal-ceramic interface by ductile rupture mechanism. In the fracture surface, the conventional ductile fracture process generated the regions with dimples. The dimples are believed to initiate at the precipitates of intermetallic phases rich in Nb and Ti (e.g., items 1 and 2 in Fig. 5a). Finally, interfacial precipitates of intermetallic phases can both embrittle the region of the $\text{Al}_2\text{O}_3/\text{Ti} + \text{Nb}/\text{Al}$ interface and plastically blunt and eliminate high stress concentrations. In the fracture surface obtained after bending test at 473 K, more dimples which are shallower and bigger than the dimples in the fracture surface after bending test at 373 K are observed. These fracture types observed in the $\text{Al}_2\text{O}_3/\text{Al}/\text{Al}_2\text{O}_3$ and $\text{Al}_2\text{O}_3/\text{Ti} + \text{Nb}/\text{Al}/\text{Ti} + \text{Nb}/\text{Al}_2\text{O}_3$ joints correspond with the bending strength results shown in Fig. 1, where the $\text{Al}_2\text{O}_3/\text{Ti} + \text{Nb}/\text{Al}/\text{Ti} + \text{Nb}/\text{Al}_2\text{O}_3$ joints generally have higher strength than $\text{Al}_2\text{O}_3/\text{Al}/\text{Al}_2\text{O}_3$ joints at elevated temperatures. Structural examinations revealed that effective reinforcement of the interfacial region of $\text{Al}_2\text{O}_3/\text{Ti} + \text{Nb}/\text{Al}/\text{Ti} + \text{Nb}/\text{Al}_2\text{O}_3$ joint, which consists of hard-and brittle-phase precipitates rich in Nb and Ti in a solid $\text{Al}(\text{Nb}, \text{Ti})$ solution with optimal plasticity,

contributes to increased mechanical strength at elevated temperatures.

4. Summary and Conclusion

The effect of a thin film Ti + Nb interlayer on the microstructure and strength of $\text{Al}_2\text{O}_3/\text{Al}/\text{Al}_2\text{O}_3$ joints at elevated temperatures is determined by the four-point bend testing, SEM, and TEM analyses.

The following conclusions were drawn:

- Better quality of $\text{Al}_2\text{O}_3/\text{Ti} + \text{Nb}/\text{Al}/\text{Ti} + \text{Nb}/\text{Al}_2\text{O}_3$ joints at elevated temperatures relative to $\text{Al}_2\text{O}_3/\text{Al}/\text{Al}_2\text{O}_3$ joints is due to specific interfacial microstructure (resulting in a solution and precipitation of rich Nb and Ti intermetallic phases) combined with plastic deformation on the metal side during fracture and leads to the production of reliable metal/ceramic joints
- Fractography of $\text{Al}_2\text{O}_3/\text{Al}/\text{Al}_2\text{O}_3$ and $\text{Al}_2\text{O}_3/\text{Ti} + \text{Nb}/\text{Al}/\text{Ti} + \text{Nb}/\text{Al}_2\text{O}_3$ joints at elevated temperatures showed that

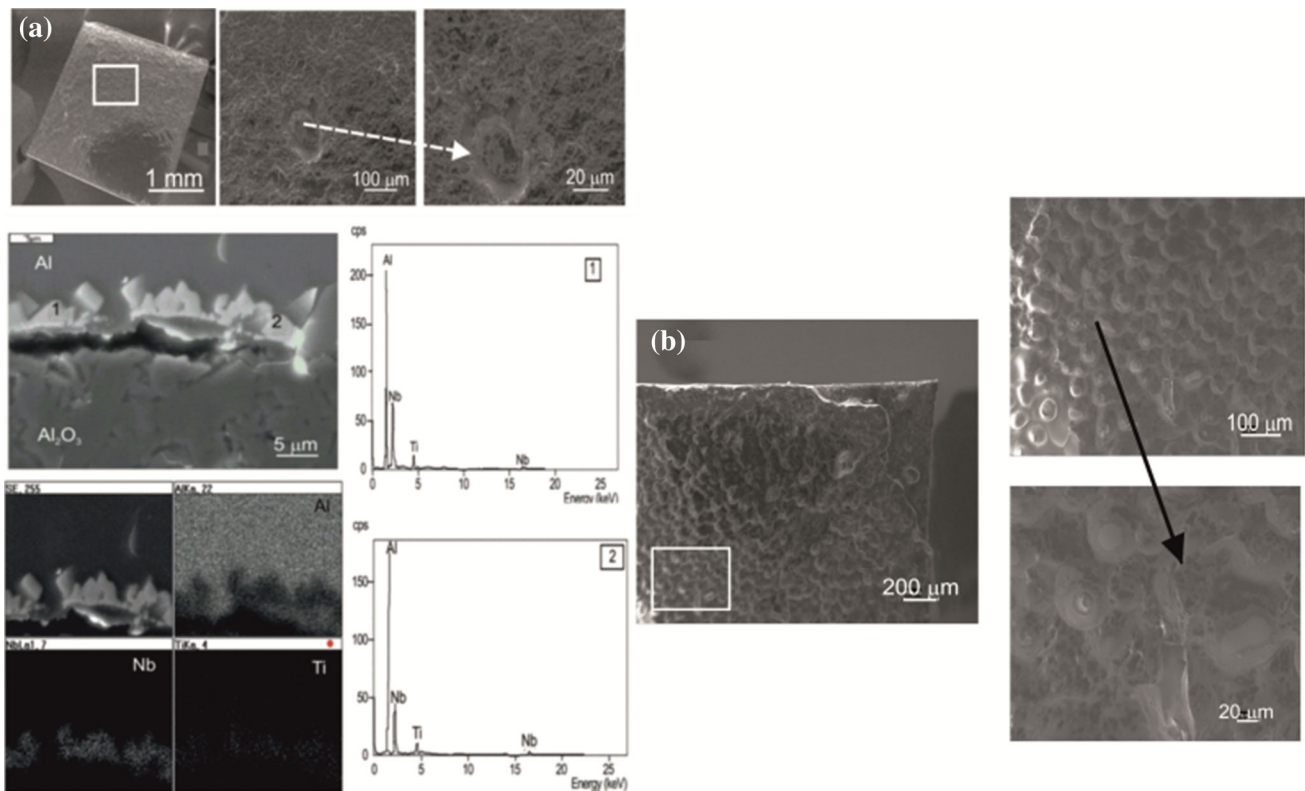


Fig. 5 SEM micrographs of fracture surface of $\text{Al}_2\text{O}_3/\text{Ti} + \text{Nb}/\text{Al}/\text{Ti} + \text{Nb}/\text{Al}_2\text{O}_3$ joints after bend test (a) at 373 K using SEM analysis of the interface with the corresponding EDS spectrum taken from the marked points 1,2, and titanium, aluminum, and niobium X-ray maps, and (b) at 473 K

failure occurred by plastic cracking in the metal near the interface. The only possible exception is $\text{Al}_2\text{O}_3/\text{Al}/\text{Al}_2\text{O}_3$ joint at 295 K, which appears to be always caused by brittle fracture of the Al_2O_3 .

Acknowledgments

This work was supported by the Ministry of Science and Higher Education under the Project No. 3T08B047 30

Open Access

This article is distributed under the terms of the Creative Commons Attribution License which permits any use, distribution, and reproduction in any medium, provided the original author(s) and the source are credited.

References

- G. Cam and M. Kocak, Progress in Joining of Advanced Metals, *Int. Mater. Rev.*, 1998, **43**(1), p 1–39
- S.B. Sinnott and E.C. Dickey, Ceramic/Metal Interface Structures and Their Relationship to Atomic- and Meso-Scale Properties, *Mater. Sci. Eng.*, 2003, **43**(1-2), p 1–59
- J.H. Selverin, F.S. Ohuchi, M. Bortz, and M.R. Notis, Interface Reactions Between Titanium Thin Films and (112) Sapphire Substrate, *J. Mater. Sci.*, 1991, **26**, p 6300–6308
- A.K. Jadan, B. Ralph, and P.R. Hornsby, Metal to Ceramic Joining via a Metallic Interlayer Bonding Technique, *J. Mater. Process. Technol.*, 2004, **152**, p 257–265
- M.L. Hattali, S. Valette, F. Ropital, N. Mesrati, and D. Treheux, Effect of Thermal Residual Stresses on the Strength for Both Alumina/Ni/Alumina and Alumina/Ni/Nickel Alloy Biomaterials, *J. Mater. Sci.*, 2009, **44**, p 3198–3210
- S.M. Hong, T.B. Reynolds, C.C. Bartlow, and A.M. Glaser, Rapid Transient-Liquid-Phase Bonding of Al_2O_3 with Microdesigned Ni/Nb/Ni Interlayers, *Int. J. Mater. Res.*, 2010, **101**(1), p 133–142
- G.P. Kelkar and A.H. Carim, Phase Equilibria in the Ti-Al-O System at 945 °C and Analysis of Ti/ Al_2O_3 Reactions, *J. Am. Ceram. Soc.*, 1995, **78**(3), p 572–576
- M. Ksiazek, M. Richert, A. Tchorz, and L. Boron, Effect of Ti, Nb, and Ti + Nb Coatings on the Bond Strength-Structure Relationship in Al/ Al_2O_3 Joints, *J. Mater. Eng. Perform.*, 2012, **21**(5), p 690–695
- A. Strecker, U. Salzberger, and J. Mayer, Specimen Preparation for Transmission Electron Microscopy: Reliable Methods for Cross-Sections and Brittle Materials, *Prakt. Metallogr.*, 1993, **30**, p 482–495
- P. Kritsalis, V. Merlin, L. Coudurier, and N. Eustathopoulos, Effect of Cr on Interfacial Interaction and Wetting Mechanism in Ni Alloy/Alumina Systems, *Acta Metall. Mater.*, 1992, **40**(6), p 1167–1174
- Ch Leinenbach, N. Werich, H.-R. Elsner, and G. Gamez, Al_2O_3 - Al_2O_3 and Al_2O_3 -Ti-Solder Joints-Influence of Ceramic Metallization and Thermal Pretreatment on Joint Properties, *Int. J. Appl. Ceram. Technol.*, 2012, **9**(4), p 751–763
- V. Raghavan, Al-Nb-Ti (Aluminium-Niobium-Titanium), *J. Phase Equilib. Diffus.*, 2005, **26**(4), p 360–368